IEEE Access
Multidisciplinary | Rapid Review | Open Access Journal

Received 26 July 2023, accepted 11 August 2023, date of publication 21 August 2023, date of current version 25 August 2023.

Digital Object Identifier 10.1109/ACCESS.2023.3307200

RESEARCH ARTICLE

A Noise Estimation Method for Hyperspectral Image Based on Stacked Autoencoder

LEI DENG[1], BING ZHOU[1], JIAJU YING[1], AND RUNZE ZHAO[2]
[1]Electronic and Optical Engineering Department, Army Engineering University of PLA, Shijiazhuang 050003, China
[2]Equipment Command and Management Department, Army Engineering University of PLA, Shijiazhuang 050003, China

Corresponding author: Bing Zhou (zhbgxgc@163.com)

ABSTRACT The imaging spectrometer is limited by a short response time and narrow channel, resulting in a low signal-to-noise ratio of hyperspectral images. The accurate estimation of noise has a significant impact on some preprocessing and downstream tasks. The existing noise estimation methods for hyperspectral images are all focused on satellite and aviation data, and there is little research on hyperspectral images with high spatial resolution. For this type of image, This article proposes a noise estimation method based on a stacked autoencoder. Firstly, the image is divided into multiple uniform regions using the K-means algorithm, and then a stacked automatic encoder is set for each uniform region. Reconstruct the spectral signal on each pixel through the corresponding stacked automatic encoder. Calculate the residual between the reconstructed image and the original image to achieve signal-to-noise separation. Finally, the image is divided into a large number of subblocks, and the subblocks containing edges are removed. The remaining subblocks are used for noise estimation in this band. The applicability of some classic noise estimation methods was experimentally tested, and the effectiveness and stability of the proposed method were verified through simulation and real data experiments.

INDEX TERMS Hyperspectral images, noise estimation, stacked autoencoder, K-means algorithm.

I. INTRODUCTION

Hyperspectral images are data cubes with high spectral resolution obtained by imaging spectrometers, which can record the two-dimensional geometric distribution of objects in the field of view and the continuous spectral curve of each pixel position [1], [2]. The detector needs to respond to hundreds of narrowband channel image signals in a short time, and the received signal energy is limited, resulting in a low signal-noise ratio of the acquired hyperspectral images. Images with low signal-noise ratio have a great impact on practical applications [3], and effective noise estimation can provide a reference for preprocessing effects such as noise removal and data dimensionality reduction, and can also be used as one of the input parameters to directly affect the algorithm effect [4], [5].

The noise in hyperspectral images is mainly composed of periodic noise and random noise, manifested as high energy values at specific frequencies in the frequency domain. It can be effectively removed through frequency domain filtering. The influence of random noise has always existed and is usually considered additive noise [6]. There are three main methods for noise estimation in remote sensing images: The laboratory method, the dark current method, and the image method. The first two methods need specific experimental conditions, and the use conditions of the image method are relatively simple. There are two main types of methods for estimating noise by image method, the idea of the first type of method is to select some uniform regions in the image and calculate the mean of the standard deviation of these uniform regions as the noise value of the band image. Fujimotor et al. initially proposed manually selecting more than four uniform areas for noise estimation [7], but it was difficult to find large uniform areas and could not be automated. Gao proposed the local mean and local standard deviations method(LMLSD), which assumes that the image is composed of a large number of uniform small blocks, and by calculating the standard deviation of these uniform subblocks as the local noise size,

The associate editor coordinating the review of this manuscript and approving it for publication was Joewono Widjaja.

and selecting the average of the local standard deviations containing the largest number of subblocks as the noise estimation of the entire image, it is inevitably affected by the subblocks containing marginal ground, resulting in erroneous noise estimates [8]. Corner et al. proposed to remove the texture information in the image by the Laplace operator and the gradient method, and then perform noise estimation [9], based on Corner's idea, the local homogeneous block standard deviations method (LHBSD) was proposed, which removes the subblocks containing the edges and then uses the remaining subblocks for noise estimation, after which the research of such spatial dimension-based methods focuses on improving the effectiveness of edge culling. The second type of effective method is based on spectral dimension, and its basic idea is to use multiple linear regression to remove highly correlated signals and use residual images to estimate noise. Roger and Arnold used this principle to first propose the spectral and spatial de-correlation method(SSDC) to estimate image noise [10], which achieved good results. To reduce the influence of inhomogeneous subblocks, the residual-scaled LMLSD (RLSD) was proposed, and the standard deviation of the residual obtained by SSDC was replaced by the local standard deviation in LMLSD for noise estimation. Gao proposed to divide the homogeneous regions according to the continuity of the spatial distribution of the features, perform multiple linear regression in each homogeneous region to obtain the residuals, and then perform noise estimation [11]. Sun proposed to use the first principal component obtained by the minimum noise fraction transformation dimensionality to determine the homogeneous region by superpixel segmentation, which provided more accurate local sample statistics, and Zhang et al. proposed to divide the homogeneous region by double determination of spectral angle distance and Euclidean distance [12], which reduced the impact of edge and texture features in the image on the estimation results. Wang et al. proposed to use a correlation vector machine to remove the nonlinear relationship between bands [13], which improved the stability of the estimate system.

Since the emergence of aerospace imaging spectrometers, noise estimation methods have been targeting hyperspectral images with low spatial resolution. With the development of detector level and the small portability of imaging spectrometer, hyperspectral images with ''dual-high-resolution'' characteristics appear in many close-range shooting applications, that is, images with high spatial resolution and high Spectral resolution [14]. The improvement of spatial resolution in hyperspectral images has brought some new problems. For example, the information on terrain features is highly detailed, and the spectral variability of the same terrain features is enhanced. Traditional methods mostly assume that the image is composed of a large number of uniform subblocks. This assumption is not valid in highly detailed hyperspectral images. The relationship between hyperspectral bands often manifests as a nonlinear relationship. The stacked autoencoder can replace linear equations and fit nonlinear functions. Moreover, its simple structure does not incur a significant computational burden. In this paper, an autoencoder-based noise estimation method is proposed for ''dual-high-resolution'' images. The K-means clustering algorithm is used to quickly divide into several types of homogeneous regions, and an autoencoder is trained in each homogeneous region to reconstruct the real signal, ultimately obtaining a residual image. To improve the stability of the method, principal component analysis is performed on the original image. Perform edge detection on the first principal component. Delete sub blocks that contain obvious edges. Calculate the standard deviation of the remaining sub blocks and sort them. Delete the top 10% and bottom 10% of the total. Use the remaining 80% as the valid value.

The remainder of this paper is organized as follows. In Section II, we described the noise characteristics of hyperspectral images. In Section III, we propose a noise estimation method and specific implementation steps based on stacked autoencoders. In Section IV, we give the selection of parameters and the experimental results and compare them with several comparison algorithms. Finally, conclusions are provided in Section V.

II. HYPERSPECTRAL IMAGE NOISE CHARACTERISTICS

A hyperspectral image is a data cube of size $M \times N \times B$, which can be seen as consisting of B grayscale images of size $M \times N$. Essentially, noise can be treated as an additional source of the signal [15], and the actual observed hyperspectral images can be described as:

$$H_k = F_k + N_k \tag{1}$$

where H_k represents the observed gray value distribution in the k-th band, F_k represents the real value of the gray value distribution in the k-th band, and N_k represents the noise distribution in the k-band.

Noise on a single image is generally assumed to consist of Gaussian noise $N_{k,g}$ and Poisson noise $N_{k,p}$, mixed noise is:

$$N_k = N_{k,g} + N_{k,p}(F_k) \tag{2}$$

The Poisson process can be regarded as a special heteroscedasticity Gaussian process [16], and the mixed noise obeys the following distribution:

$$N_k \sim \mathcal{N}\left(0, \sigma_{k,g}^2 + \sigma_{k,p}^2 F_k\right) \tag{3}$$

where $\sigma_{k,g}^2$ is the variance of $N_{k,g}$ and $\sigma_{k,p}^2$ is the variance of $N_{k,p}$, $\mathcal{N}$ denote normal distributions.

The standard deviation of the final mixed noise in the k-band is:

$$\sigma_k = \sqrt{\sigma_{k,g}^2 + \sigma_{k,p}^2 F_k} \tag{4}$$

For hyperspectral images, images in each band can be treated as a single static image [17], with different sizes of noise in different bands.

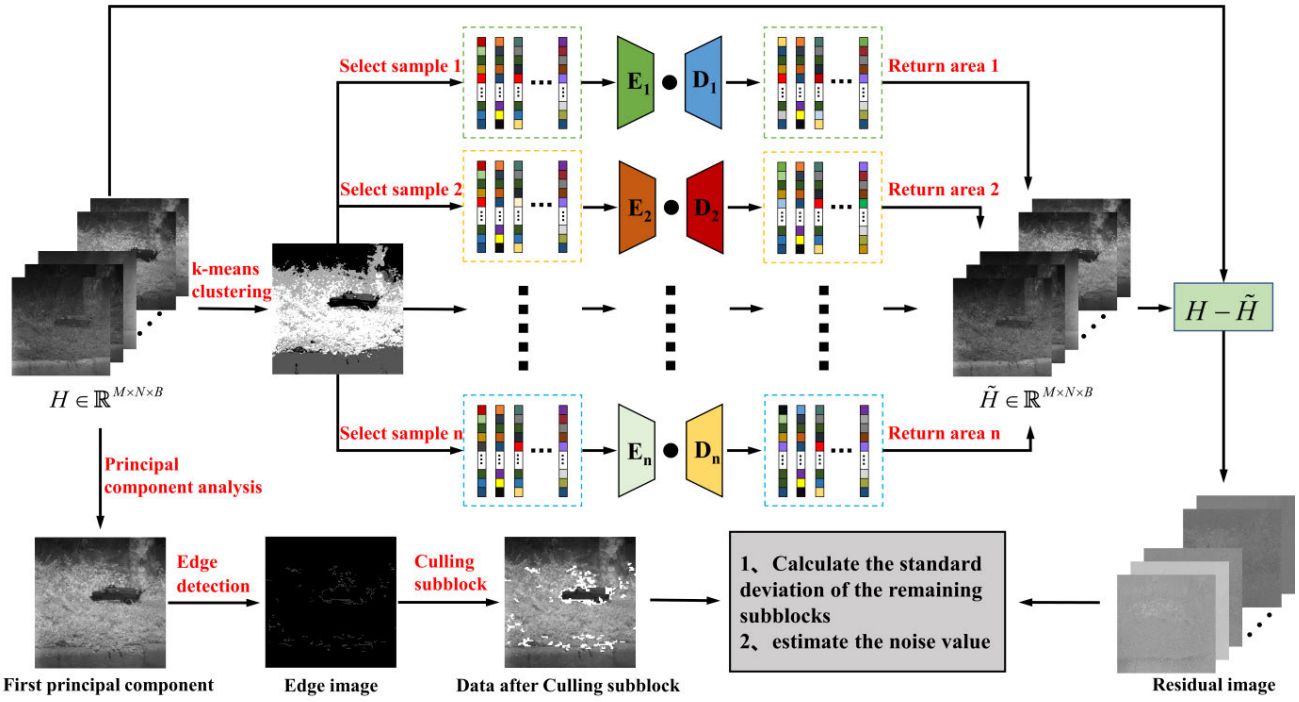

FIGURE 1. Flowchart of the proposed method.

III. PROPOSED METHOD

In this section, we describe how to achieve hyperspectral noise estimation using autoencoders. The method in this paper is mainly composed of the following parts: (1) K-means algorithm for classification; (2) The autoencoder is used to reconstruct the image in each homogeneous region; (3) The reconstructed image is different from the original image to achieve signal-to-noise separation; (4) Divides the original image into a large number of subblocks, detect the edges of the original image, and remove the subblocks that contain the edges; (5) the standard deviation of the remaining subblocks is calculated and the noise value is estimated. Fig.1 shows the overall flow of the method.

A. HOMOGENEOUS REGION SELECTION

K-means can easily and quickly divide hyperspectral images into several homogeneous regions. The principle is to randomly select k pixels as the initial clustering center. Classify the remaining pixels into the class with the smallest distance and update the cluster center. Complete clustering without reallocating pixels or reaching the maximum number of iterations. The handheld imaging spectrometer has a smaller field of view and contains fewer ground objects. The value of k is generally between 2 and 4. Algorithm 1 provides the specific process of implementing K-means clustering in hyperspectral images.

Measure the distance between pixels and class centers using Euclidean distance. The pixels in the final hyperspectral image are divided into several categories.

Algorithm 1 K-means clustering

1. Input hyperspectral image $H \in \mathbb{R}^{M\times N\times B}$
2. Randomly select k pixels $a_1^{(1)}, a_2^{(1)}, \cdots, a_k^{(1)}$ as the initial cluster center
3. The distance from the pixel to the center of the cluster is calculated as follows: $dist_{i,j}^{(1)} = \left\| h_i - a_j^{(1)} \right\|_2$, And put it in the closest category.
4. Recalculate the cluster centers for each category as follows: $a_j^{(2)} = \frac{1}{|S_j|} \sum_{h\in S_j} h$
5. Repeat steps 3, 4 until the termination condition is reached

B. CORRELATION REMOVAL

Each pixel on a hyperspectral image is a nearly continuous spectral curve with strong correlations in adjacent bands, in fact, this correlation often appears as a nonlinear relationship. When the autoencoder obtains raw and closed inputs, the hidden layer can perform well in encoding, and the stacked autoencoder composed of multiple autoencoders has better performance [18]. A stacked autoencoder is an unsupervised neural network model that learns the implicit features of the input data, intending to restore the original data. Stacked autoencoders are used to reconstruct real signals in homogeneous regions to achieve signal-to-noise separation. The training process of the stacked autoencoder is shown in Fig.2.

An autoencoder is essentially a three-layer neural network, which is an input layer, a hidden layer, and a reconstruction layer. By minimizing the error of the input layer and

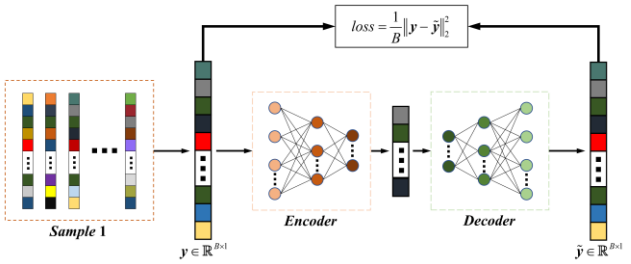

FIGURE 2. Training process of stacked autoencoders.

the reconstruction layer, the deep features of the data are generated in the hidden layer. The loss function is defined as the mean squared error of input and reconstruction, as shown in the following formula:

$$loss = \frac{1}{B}\|y - \tilde{y}\|_2^2 \tag{5}$$

The input is mapped to the hidden layer through the ''encoder'', and the hidden layer data is implicitly projected to the reconstruction layer through the ''decoder''. A stacked autoencoder is a superposition of multiple autoencoders. Its training is layer-by-layer, not directly training the entire network. For coding networks with L-layers, the network structure is trained as follows: $d^{(0)} \rightarrow d^{(1)} \rightarrow \cdots \rightarrow d^{(L)}$. The first step is to complete the training of $d^{(0)} \rightarrow d^{(1)}\& \rightarrow \tilde{d}^{(0)}$, and obtain the network parameters $W^{(1)}$ and $b^{(1)}$ of the first layer. $\tilde{d}^{(\cdot)}$ is the reconstruction layer of $d^{(\cdot)}$. Then carry out training for $d^{(1)} \rightarrow d^{(2)} \rightarrow \tilde{d}^{(1)}$ and continue until the end of training for $d^{(L)} \rightarrow d^{(L-1)} \rightarrow \tilde{d}^{(L)}$. Ultimately, all network parameters are stacked into a stacked autoencoder.

Encoder and Decoder have the same number of layers, symmetrical left and right. The parameters of the symmetry layer can also have a transpose relationship, which can halve the parameters of the model, speed up training and reduce the risk of overfitting. The l-layer output of the stacked autoencoder is:

$$y^{(l)} = f\left(W^{(l)}y^{(l-1)} + b^{(l)}\right) \tag{6}$$

It is worth noting that training and reconstruction are whole, and each input data undergoes training and reconstruction. Every time noise estimation is performed, an untrained model is used. The reconstructed spectral curve on each pixel is reassigned to the original position to generate the reconstructed image $\tilde{H}$. The original image and the reconstructed image are subtracted to obtain the residual image: $\Delta H = H - \tilde{H}$, which achieves signal-noise separation.

C. EDGE CULLING

To mitigate the effects of texture information, remove edges from the image. First, principal component analysis was performed on H, the first principal component is used for edge detection. Edge detection is done by the Canny operator.

Algorithm 2 Estimation of noise value in the b-th band

1. Input $R \in \mathbb{R}^{B\times R\times C\times h\times w}$ and $\hat{E} \in \mathbb{R}^{R\times C\times h\times w}$
2. **for** $(i, j) = 1$ to (R, C)
   for $(m, n) = 1$ to (h, w)
   if $\hat{E}\,(i, j, m, n) = 1$
   $R_b\,(i, j) = O$
   end
   end
   end
3. **for** $(i, j) = 1$ to (R, C)
   if std $R_b\,(i, j) \neq 0$
   add std $R_b\,(i, j)$ **to** v_b
   end
   end
4. **Sort** $v_b, (1, p) =$ **size**(v_b).
5. $\hat{v}_b = v_b\,(0.1p : 0.9p)$
6. $n =$ **mean**$(\hat{v}_b)$

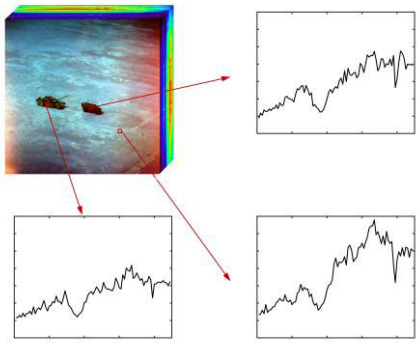

FIGURE 3. Spectral curves extracted from real datae.

The operator first uses a Gaussian smoothing filter to smooth the image to remove noise, and uses a finite difference of first-order bias to calculate the gradient amplitude and direction. In the process of processing, it will also go through a process of non-maximum suppression and finally use two thresholds to connect the edges and output a binary image $E \in \mathbb{R}^{M\times N}$.

Divide residual image ΔH evenly into residual subblock data $R \in \mathbb{R}^{B\times R\times C\times h\times w}$, divide edge image E evenly into edge subblock data $\hat{E} \in \mathbb{R}^{R\times C\times h\times w}$. Where B is the number of bands; h, w is the size of the subblock; R is the number of subblocks on each column, and C is the number of subblocks on each row.

Algorithm 2 gives the pseudocode to obtain the noise estimate of the b-th band. This process will be repeated in other bands.

IV. EXPERIMENT AND ANALYSIS

A. DATA DESCRIPTION

Experiments were performed using two types of data to compare noise estimate methods. The first is simulated data that is considered synthesis, and the second is real hyperspectral data.

TABLE 1. MEAP between estimated and real values.

Simulation image	Method	MEAP(%)				
		SNR=−10 dB	SNR=0 dB	SNR=10 dB	SNR=20 dB	SNR=30 dB
Homogenou	Proposed method	0.81	0.59	0.48	0.69	0.92
	SSDC	0.12	0.13	0.11	0.12	0.12
	LMLSD	3.56	4.65	3.08	6.11	3.67
	LHBSD	4.01	12.75	9.32	7.42	15.19
	RLSD	6.67	13.22	4.58	5.46	4.69
Sparse subblock	Proposed method	0.67	0.65	0.49	0.51	0.36
	SSDC	0.13	0.18	0.74	0.83	0.82
	LMLSD	6.92	5.76	3.25	7.11	6.05
	LHBSD	10.33	6.30	7.74	5.83	6.91
	RLSD	5.33	9.84	8.10	14.46	47.18
Dense fringe	Proposed method	0.87	0.54	0.59	0.63	0.58
	SSDC	0.13	0.97	9.45	12.98	13.10
	LMLSD	5.06	6.87	8.72	15.13	15.58
	LHBSD	7.85	9.26	4.54	30.63	27.44
	RLSD	5.86	9.89	9.17	14.64	25.91
Dense subblock	Proposed method	0.57	0.43	0.57	0.49	0.48
	SSDC	0.15	0.65	6.38	12.21	14.37
	LMLSD	5.21	5.75	4.99	8.95	3.64
	LHBSD	6.10	9.26	5.89	8.69	4.56
	RLSD	8.97	3.29	15.38	24.92	52.15

1) SIMULATED DATA

The spectral curves of three features were selected from the real hyperspectral image to synthesize the simulation image, and the three curves selected were shown in Fig.3.

Add white Gaussian noise to the analog image according to a certain signal-to-noise ratio, which in this paper is defined as:

$$SNR = 10\lg \frac{u_p}{\sigma_p} \tag{7}$$

where u_p is the grayscale mean of the p-band and σ_p is the standard deviation of the Gaussian white noise added in the p-band.

The simulated hyperspectral data is 600 × 600 × 89 pixels in size and is added with the noise of 15 dB, 20 dB, and 25 dB. Fig.4 shows four different spatial distributions of the simulated data. Fig.4(a) is hyperspectral data consisting of only one spectrum. Fig.4(b) Hyperspectral data with sparse subblocks synthesized from three spectra with a subblock size of 200 × 200 pixels. Fig.4(c) is a synthesis of hyperspectral data with denser fringes from three spectra with a fringe height of 10 pixels. Fig.4(d) is hyperspectral data synthesized by three spectra with a denser subblock size of 10 × 10 pixels. The different color blocks in the figure represent different spectra.

2) REAL DATA

Fig.5 shows three hyperspectral images acquired at different times and places, all with a size of 1000 × 1000 × 89 pixels and a wavelength range of 449nm-801nm. Images

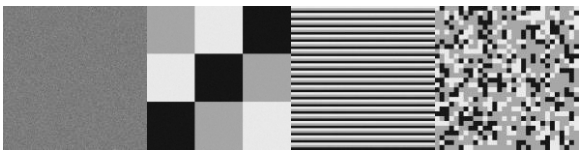

FIGURE 4. Spatial distribution of simulated data. (a) homogeneous (b) sparse subblock (c) dense fringe (d) dense subblock.

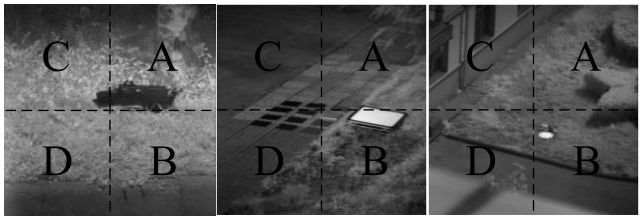

FIGURE 5. Spatial distribution of real data.(a) Data 1 (b) Data 2 (c) Data 3.

are taken at close range with high spatial resolution. Each real hyperspectral image will be divided into four sub-images A, B, C, and D of size 500 × 500 × 89, and the four sub-images can be regarded as obtained in the same experiment and should have the same noise.

B. PARAMETER SETTINGS

The methods for conducting experiments are this method, LMLSD, LHBSD, SSDC, and RLSD. According to the tips of

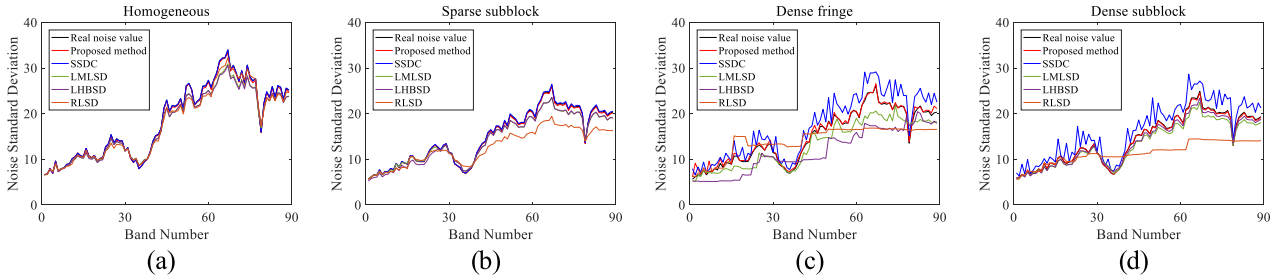

FIGURE 6. Noise estimate results on the simulated data. (a) homogeneous (b) sparse subblock (c) dense fringe (d) dense subblock.

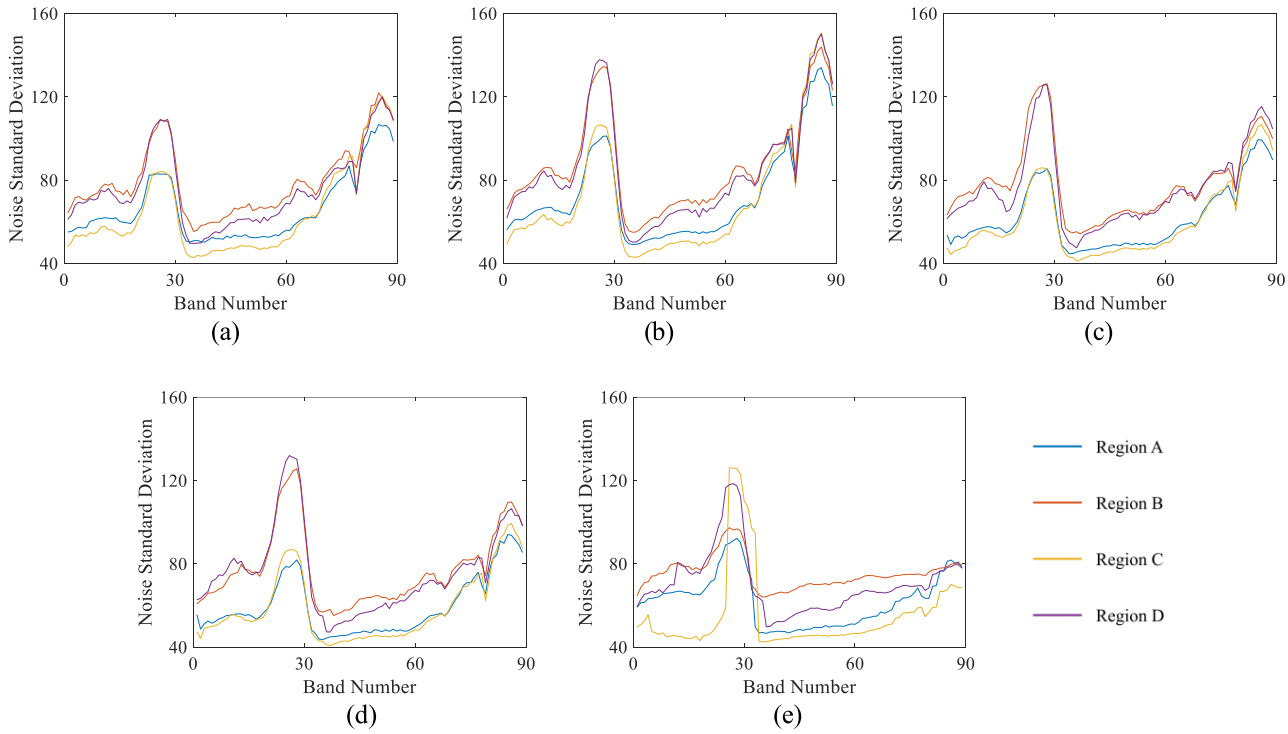

FIGURE 7. Noise estimation result for Data 1. (a) proposed method (b) SSDC (c) LMLSD (d) LHBSD (e) RLSD.

the literature [6], the subblock size of LMLSD and LHBSD is set to 4×4, and the edge detection operator in LHBSD adopts the canny operator. The subblock size of SSDC and RLSD is set to 15×15. In this article method, the input layer dimension of the stacked autoencoder is 89, the dimensions of the hidden layers of the three layers are set to 50, 30, and 50, the dimension of the reconstruction layer is 89, the subblock size is selected as 10×10, and the edge detection part is completed by the canny operator.

C. RESULTS AND ANALYSIS

1) RESULTS AND ANALYSIS OF SIMULATED DATA

The noise estimates for each method on the simulated data will be compared with the real noise values. The experimental results on simulated data with 20 dB of noise are shown in Fig.6. The estimated error on each SNR data is quantified in Table 1 using the mean absolute percentage error (MEAP).

For homogeneous simulated data, most of the MEAP of the noise estimation values of the five methods mentioned in the paper are below 10%, which can accurately evaluate the noise. From the comparison between the various methods, whether it is homogeneous data or complex data, LMLSD, LHBSD, and RLSD perform noise estimate effects that are not as good as the proposed method and SSDC. When evaluating homogeneous data, SSDC performed better than the method here, but the MEAP were all below 1%, and there was no significant difference. When the image has a dense texture, the MEAP between the noise estimation value and the real value of the method in this paper is still less than 1%, while the noise estimation value of other methods has a slightly larger deviation, reaching 10%. The estimate of SSDC in Fig.6(c) and Fig.6(d) shows a jagged overall appearance and a large deviation from the noise real value, indicating that complex textures have a great influence on

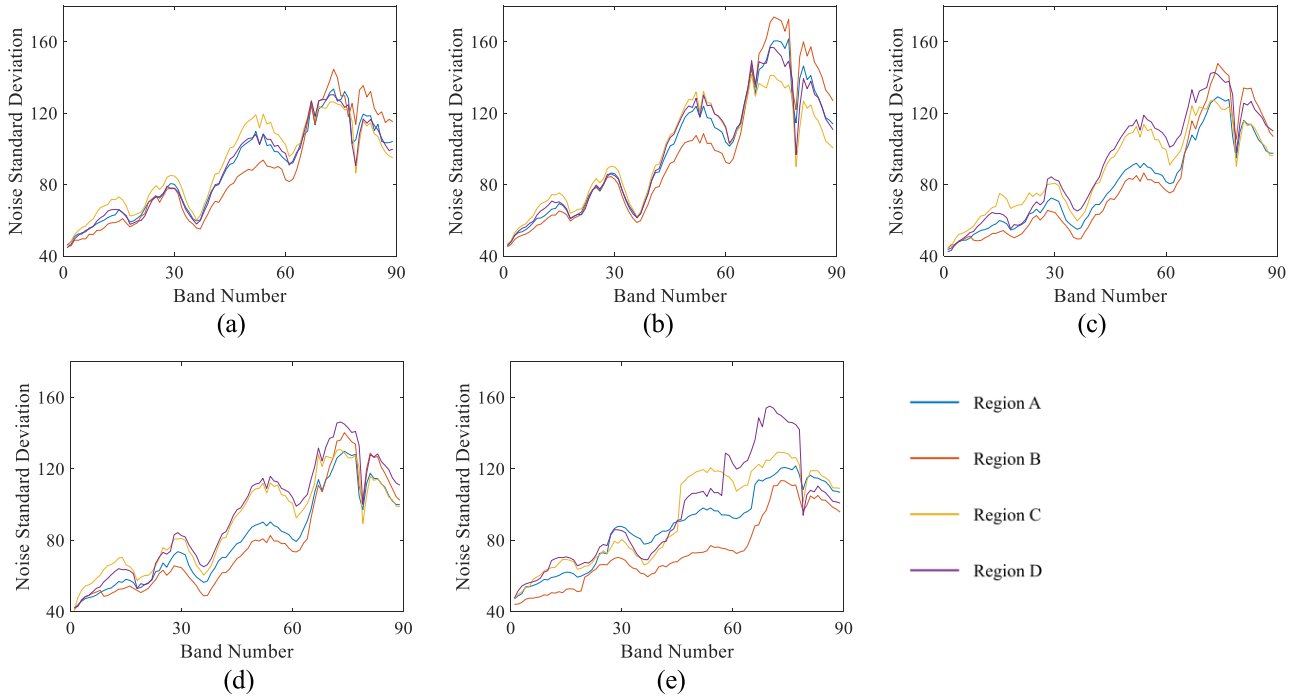

FIGURE 8. Noise estimation result for Data 2. (a) proposed method (b) SSDC (c) LMLSD (d) LHBSD (e) RLSD.

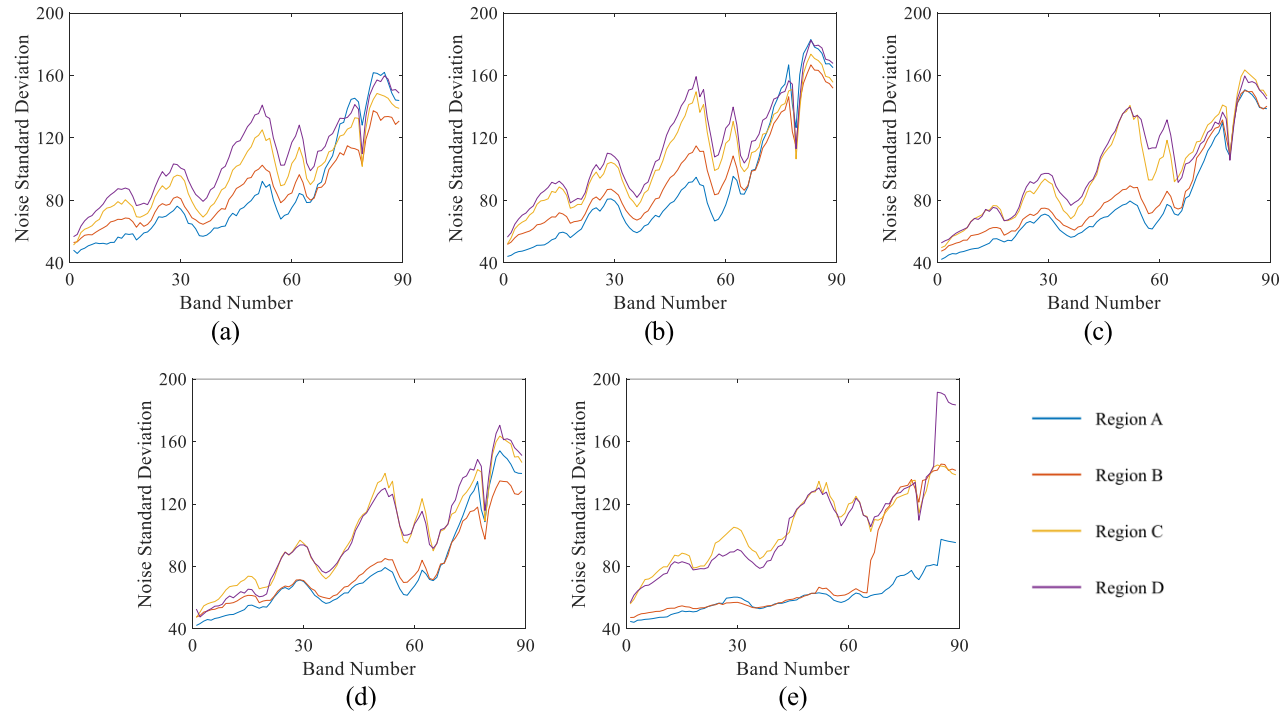

FIGURE 9. Noise estimation result for Data 3. (a) proposed method (b) SSDC (c) LMLSD (d) LHBSD (e) RLSD.

SSDC. The proposed method performs better than SSDC in estimating complex scenarios. Experiments also show that single-direction texture and multi-directional texture have no almost effect on the estimation effect of the proposed method. The signal-to-noise ratio has a significant impact on all four comparison algorithms. Although the error of the proposed

TABLE 2. SMEAP between each regions.

Simulation image	Method	SMEAP(%)						Mean(%)
		A&B	A&C	A&D	B&C	B&D	C&D	
Data 1	Proposed method	18.71	7.97	13.33	23.33	5.80	18.07	14.53
	SSDC	18.68	7.51	15.34	23.46	4.59	19.23	14.80
	LMLSD	25.60	12.27	15.73	37.55	10.66	27.18	21.50
	LHBSD	25.92	11.69	13.67	37.13	13.21	24.22	20.97
	RLSD	27.66	14.16	19.12	41.32	32.98	17.08	25.38
Data 2	Proposed method	8.12	6.53	2.46	14.04	8.92	5.81	7.65
	SSDC	7.04	6.83	2.94	13.57	9.30	4.73	7.40
	LMLSD	8.46	14.17	6.01	13.23	10.32	14.50	11.12
	LHBSD	7.24	8.96	10.55	11.43	8.51	13.15	9.97
	RLSD	17.69	17.56	13.66	13.91	9.09	12.62	14.09
Data 3	Proposed method	13.37	21.43	28.79	12.44	22.10	9.83	17.99
	SSDC	13.60	25.89	30.08	14.21	20.06	6.11	18.32
	LMLSD	12.27	38.14	41.62	27.42	30.73	5.99	26.03
	LHBSD	9.72	31.71	40.05	23.65	31.71	10.01	24.47
	RLSD	12.99	51.88	44.92	45.11	37.69	9.40	33.67

method slightly increases with the decrease of signal-to-noise ratio, it remains below 1%, which can still be considered as having low sensitivity to signal-to-noise ratio.

2) RESULTS AND ANALYSIS OF REAL DATA

In each data, noise estimation is carried out for its four regions A, B, C, and D. The experimental results corresponding to the three hyperspectral images are shown in Fig.7, Fig.8, and Fig.9. The error between the two estimation curves was measured using symmetric mean absolute percentage error (SMEAP), and the average value was used to describe the overall error of the four estimation curves, as shown in Table 2.

The results in Table 2 show that the proposed method and SSDC are superior to other methods in the stability and robustness of noise estimation, and this method is only slightly ahead of SSDC. Due to the effect of H_2O in the atmosphere, an obvious absorption peak in the image spectrum used in the experiment is located near the 79th band, and the estimated curve of the proposed method is more stable than that of other methods. The A and C, B and D regions of data 1 contain similar features and similar proportions. The result is that the estimation error between A and C, B and D is small, and if they are not similar, the error is large. The experiments of the other two groups of data have similar phenomena, indicating that the type and proportion of feature distribution have a certain degree of influence on the estimation effect. An interesting phenomenon is that the difference between RLSD and SSDC is only the last effective value-taking strategy. According to the experimental results, the effect of RLSD is very poor, and this effective value-taking strategy may not be suitable for hyperspectral images with high spatial resolution. From the perspective of overall experiments, there are many fine and dense textures in hyperspectral images with high spatial resolution. The texture of natural objects is more complex than that of artificial objects, which has a great impact on the effect of noise estimation.

V. CONCLUSION

In this paper, a new method for hyperspectral image noise estimation is proposed. K-means is used to divide homogeneous regions, and the powerful reconstruction capability of stacked autoencoders is used to achieve signal-noise separation. Experiments on the simulated data show that the method can estimate the noise well with different signal-noise ratios. Experiments on three true hyperspectral images show that the stability and robustness of the proposed method are superior to other methods in the case of high spatial resolution. This paper does not try other clustering algorithms, and better clustering algorithms may improve the reduction effect of stack autoencoders for homogeneous regions. Furthermore, generalizing the proposed method to specific applications of noise removal will be the focus of our future work.

REFERENCES

[1] Tuya, "Graph convolutional enhanced discriminative broad learning system for hyperspectral image classification," *IEEE Access*, vol. 10, pp. 90299–90311, 2022.
[2] F. Ma, S. Liu, F. Yang, and G. Xu, "Piecewise weighted smoothing regularization in tight framelet domain for hyperspectral image restoration," *IEEE Access*, vol. 11, pp. 1955–1969, 2023.
[3] T. Qingxi, Z. Bing, and Z. Lifu, "Current progress of hyperspectral remote sensing in China," *J. Remote Sens.*, vol. 20, no. 5, pp. 689–707, Sep. 2016.
[4] J. M. Bioucas-Dias and J. M. P. Nascimento, "Hyperspectral subspace identification," *IEEE Trans. Geosci. Remote Sens.*, vol. 46, no. 8, pp. 2435–2445, Aug. 2008.
[5] C. Li, Y. Ma, X. Mei, F. Fan, J. Huang, and J. Ma, "Sparse unmixing of hyperspectral data with noise level estimation," *Remote Sens.*, vol. 9, no. 11, p. 1166, Nov. 2017.
[6] B. Zhang and L. R. Gao, "Hyperspectral image noise evaluation and data dimensionality reduction," in *Hyperspectral Image Classification and Target Detection*, 1st ed. China, East Asia: Science Press, 2011, pp. 25–51.

[7] N. Fujimotor, Y. Takahashi, T. Moriyama, M. Shimada, H. Wakabayashi, Y. Nakatani, and S. Obayashi, "Evaluation of spot hrv image data received in Japan," in *Proc. 12th Can. Symp. Remote Sens. Geosci. Remote Sens. Symp.*, Vancouver, BC, Canada, Jul. 1989, pp. 463–466. [Online]. Available: https://ieeexplore.ieee.org/document/578740
[8] B.-C. Gao, "An operational method for estimating signal to noise ratios from data acquired with imaging spectrometers," *Remote Sens. Environ.*, vol. 43, no. 1, pp. 23–33, Jan. 1993.
[9] B. R. Corner, R. M. Narayanan, and S. E. Reichenbach, "Noise estimation in remote sensing imagery using data masking," *Int. J. Remote Sens.*, vol. 24, no. 4, pp. 689–702, Jan. 2003.
[10] R. E. Roger and J. F. Arnold, "Reliably estimating the noise in AVIRIS hyperspectral images," *Int. J. Remote Sens.*, vol. 17, no. 10, pp. 1951–1962, Jul. 1996.
[11] L.-R. Gao, B. Zhang, X. Zhang, W.-J. Zhang, and Q.-X. Tong, "A new operational method for estimating noise in hyperspectral images," *IEEE Geosci. Remote Sens. Lett.*, vol. 5, no. 1, pp. 83–87, Jan. 2008.
[12] L. F. Zhang, X. H. Lu, Y. Cen, and X. J. Sun, "Optimized spatial and spectral decorrelation method for noise estimation in hyperspectral images," *J. Remote Sens.*, vol. 25, no. 7, pp. 1411–1421, Jul. 2021.
[13] X. F. Wang, C. L. Hou, Q. J. Yan, J. P. Zhang, and A. H. Wang, "Noise estimation algorithm based on relevance vector machine for hyperspectral imagery," *Infr. Laser Eng.*, vol. 43, no. 12, pp. 4159–4163, 2014.
[14] J. Qu, Y. Li, Q. Du, and H. Xia, "Hyperspectral and panchromatic image fusion via adaptive tensor and multi-scale Retinex algorithm," *IEEE Access*, vol. 8, pp. 30522–30532, 2020.
[15] X. Sun, "Research on remote sensing image noise evaluation method and system implementation," M.S. thesis, Nanjing Univ. Sci. Technol. Nanjing, China, 2018.
[16] A. Foi, M. Trimeche, V. Katkovnik, and K. Egiazarian, "Practical Poissonian–Gaussian noise modeling and fitting for single-image raw-data," *IEEE Trans. Image Process.*, vol. 17, no. 10, pp. 1737–1754, Oct. 2008.
[17] L. Sun, B. Li, and Y. Nian, "Superpixel-based mixed noise estimation for hyperspectral images using multiple linear regression," *Remote Sens.*, vol. 12, no. 8, p. 1324, Apr. 2020.
[18] S. Singh and S. S. Kasana, "Efficient classification of the hyperspectral images using deep learning," *Multimedia Tools Appl.*, vol. 77, no. 20, pp. 27061–27074, Oct. 2018.

LEI DENG was born in Jiujiang, Jiangxi, China, in 2000. He received the bachelor's degree in optical engineering from the Army Engineering University of PLA, in 2021, where he is currently pursuing the master's degree in optical engineering. His research interest includes hyperspectral image processing.

BING ZHOU received the Ph.D. degree from the Shijiazhuang Mechanical Engineering College, Shijiazhuang, China, in 2006. He is currently a Professor with the Army Engineering University of PLA, Shijiazhaung. His research interests include photoelectric countermeasure and information engineering.

JIAJU YING received the Ph.D. degree from the Shijiazhuang Mechanical Engineering College, Shijiazhuang, China, in 2009. He is currently a Lecturer with the Army Engineering University of PLA, Nanjing, China. He has authored more than 30 technical papers. His teaching and research interests include digital image processing and laser system design.

RUNZE ZHAO received the bachelor's degree in vehicle engineering from Shijiazhuang Mechanical Engineering College, Shijiazhuang, China, in 2016. He is currently pursuing the master's degree in engineering management with the Equipment Command and Management Department, Army Engineering University of PLA. His research interests include vehicle powertrains and optoelectronic countermeasures technology.